Contents lists available at ScienceDirect

Saudi Pharmaceutical Journal

journal homepage: www.sciencedirect.com

Original article

Compatibility study of rosmarinic acid with excipients used in pharmaceutical solid dosage forms using thermal and non-thermal techniques

Kleyton Santos Veras [a], Flávia Nathiely Silveira Fachel [a], Vanessa Pittol [a], Keth Ribeiro Garcia [a], Valquíria Linck Bassani [a], Venina dos Santos [b], Amélia Teresinha Henriques [a], Helder Ferreira Teixeira [a], Letícia Scherer Koester [a,*]

[a] Programa de Pós-Graduação em Ciências Farmacêuticas, Faculdade de Farmácia, Universidade Federal do Rio Grande do Sul, Avenida Ipiranga, 2752, 90610-000 Porto Alegre, Brazil
[b] Programa de Pós-Graduação em Engenharia de Processos e Tecnologias, Universidade de Caxias do Sul, Rua Francisco Getúlio Vargas, 1130, 95070-560 Caxias do Sul, RS, Brazil

A B S T R A C T

Rosmarinic acid (RA) is a phenolic compound that presents well-documented anti-inflammatory, antioxidant and antitumor activities, and based on its pharmacological potential and poor bioavailability, several solid dosage forms have been developed to RA delivery. Therefore, in literature, there are no reports about RA compatibility with excipients. In this regard, the aim of the present study was to evaluate, for the first time, the compatibility of RA with excipients commonly used in solid dosage forms at a 1:1 (RA: excipient) ratio using differential scanning calorimetry (DSC), thermogravimetry (TG), Fourier-transform infrared (FTIR), solid-state nuclear magnetic resonance (ssNMR), and isothermal stress testing (IST) coupled with liquid chromatography (LC). The excipients selected were hydroxypropyl methylcellulose (HPMC), microcrystalline cellulose (MCC), lactose monohydrate (LAC), polyvinylpyrrolidone (PVP), talc (TALC), croscarmellose sodium (CCS), and magnesium stearate (MgSTE). According to DSC results, physical interactions were found between RA and HPMC, LAC, CCS, and MgSTE. The TG analyses confirmed the physical interactions and suggested chemical incompatibility. FTIR revealed physical interaction of RA with TALC and MgSTE and the ssNMR confirmed the physical interaction showed by FTIR and excluded the presence of chemical incompatibility. By IST, the greatest loss of RA content was found to CCS and MgSTE (>15%), demonstrating chemical incompatibilities with RA. High temperatures used in DSC and TG analyses could be responsible for incompatibilities in binary mixtures (BMs) with HPMC and LAC, while temperature above 25 °C and presence of water were factors that promote incompatibilities in BMs with CCS and MgSTE. Overall results demonstrate that RA was compatible with MCC and PVP.

© 2019 The Authors. Production and hosting by Elsevier B.V. on behalf of King Saud University. This is an open access article under the CC BY-NC-ND license (http://creativecommons.org/licenses/by-nc-nd/4.0/).

1. Introduction

Rosmarinic acid (RA), an ester derived from caffeic acid, is a hydroxycinnamic acid (Fig. 1) commonly found in vegetal species from Lamiaceae family such as *Rosmarinus officinalis*, *Melissa offic-inalis,* and *Perilla frutescens*. RA is an important natural resource due to its well-documented anti-inflammatory, antioxidant, and antitumor activities (Amoah et al., 2016; Fachel et al., 2019). Based on the pharmacological potential of RA and its poor bioavailability, some solid dosage forms have been proposed for RA delivery, such as cyclodextrins complexes and lipid-nanotechnology-based delivery systems (Campos et al., 2014; Madureira et al., 2015; Veras et al., 2019).

In this context, the drug-drug or drug-excipient compatibility is an important field of study to be carried out prior to the formulation of a dosage form in order to predict physical and chemical interactions or incompatibilities that may affect the safety and effectiveness of the drug (Bezerra et al., 2017; de Oliveira et al., 2017). Physical interactions may promote changes in appearance, drug release profile, polymorphic form, taste, odor, or solubility,
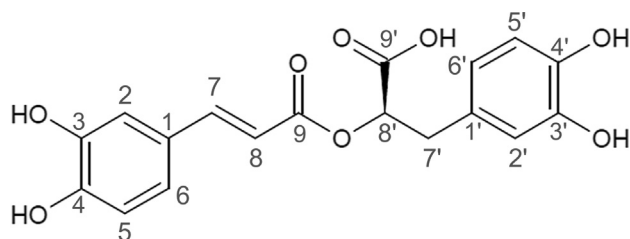
Fig. 1. Rosmarinic acid chemical structure and carbons assignments.

while chemical incompatibilities are related to drug degradation, resulting in loss of drug potency and the possibly formation of other molecules (Narang et al., 2012).

Several techniques have been applied in compatibility studies with excipients, such as differential scanning calorimetry (DSC), thermogravimetry (TG), Fourier-transform infrared (FTIR), X-ray diffraction (XRD), solid-state nuclear magnetic resonance (ssNMR) and isothermal stress testing (IST) coupled with liquid chromatography (LC) (Chadha and Bhandari, 2014). Some of these techniques are more commonly used due to fast analyses, low material consumption, and the ability to detect impurities/degradation products (Chadha and Bhandari, 2014; Pires et al., 2017; Rojek et al., 2013; Verma and Garg, 2005).

Among hydroxycinnamic acids, only ferulic acid has been studied with respect to drug-excipients compatibility, but this compound is concerned with topical excipients (Bezerra et al., 2017). Razboršek (2011) demonstrated the stability of RA powder under different conditions, but its compatibility with excipients employed in the formulation of solid dosage forms remains unexplored. Hence, the aim of the present study was to evaluate, for the first time, the compatibility of RA with excipients commonly used in solid dosage forms, by DSC, TG, FTIR, ssNMR and IST.

2. Materials and methods

2.1. Materials

The following chemicals were employed: rosmarinic acid standard (96% purity) (Sigma-Aldrich, Slovakia); hydroxypropyl methylcellulose (Methocel™ DC, Colorcon) (HPMC); microcrystalline cellulose (Microcel®, Blanver) (MCC); lactose monohydrate (Delaware) (LAC); polyvinylpyrrolidone (Kollidon® CL-M, BASF) (PVP); talc (Delaware) (TALC); croscarmellose sodium (Solutab® A, Blanver) (CCS), and magnesium stearate (Acros Organics) (MgSTE). The excipients and their respective classification are shown in Table 1 (Rowe et al., 2012).

2.2. Methods

2.2.1. Binary mixtures (BMs)

RA and excipients were passed through a 60-mesh size sieve, and BMs of RA with each excipient were prepared at a 1:1 (w/w)

Table 1
Excipients used in the compatibility study.

Excipient	Classification
HPMC	Binder, polymer for film-coating, and as a matrix for use in extended release tablet formulations
MCC	Adsorbent, tablet and capsule diluent; tablet disintegrant
LAC	Binder, filler-binder, and flow aid in direct compression tableting
PVP	Tablet disintegrant and dissolution agent
TALC	Anticaking agent; glidant; tablet and capsule diluent; tablet and capsule lubricant
CCS	Disintegrant agent
MgSTE	Tablet and capsules lubrificant agent

ratio by vortex mixing for 5 min. The BMs were added to glass vials protected from light. 1:1 (w/w) ratio BM of RA and excipients was selected to maximize the chance of observing any drug–excipient interaction.

2.2.2. Differential scanning calorimetry (DSC)

The DSC analysis were performed in a DSC-60 calorimeter (Shimadzu Co., Kyoto, Japan) using the following conditions: dynamic nitrogen atmosphere of 50 mL min^{-1} and a heating rate of 10 °C min^{-1}. The DSC was calibrated with indium (156.6 °C) and zinc (419.6 °C) as standards. The RA, excipients, and BMs were accurately weighed and submitted to further heat scanning from 15 to 400 °C in a sealed aluminum pan. An empty, sealed aluminum pan was used as a reference. Curves were then analyzed for the presence of interactions. Data analysis was carried out using TA 60 Analysis software.

2.2.3. Thermogravimetry (TG)

The TG analysis were performed using a TGA-50 (Shimadzu Co., Kyoto, Japan) under the following conditions: dynamic nitrogen atmosphere of 50 mL min^{-1} and a heating rate of 10 °C min^{-1}. The TGA-50 was calibrated with calcium oxalate as standard. The RA and BMs with HPMC, LAC, CCS and MgSTE were accurately weighed and submitted to further heat scanning until 900 °C in a sealed aluminum pan. Data analysis and derivative thermogravimetric (DTG) curves were carried out using the TA 60 analysis software.

2.2.4. Fourier-transformed infrared (FTIR)

Infrared spectra covering the range of 600–4000 cm^{-1} were obtained for the RA, excipients, and BMs with a Spectrum BX FTIR spectrometer with a MIRacle ATR accessory (Perkin Elmer, MA, USA). Spectra obtained were the average of 40 scans at a resolution of 4 cm^{-1}.

2.2.5. Solid-state nuclear magnetic resonance (ssNMR)

Solid-state ^{13}C CP/MAS NMR analyses were carried out on an Agilent DD2/ Narrow Bore 500 MHz spectrometer with 4 mm probe, operating at 499.84 MHz (^{1}H) and 125.70 MHz (^{13}C), using 90° pulse width 2.90 μs (^{1}H) and 2.79 μs (^{13}C), delay 5 s, 7 ms contact time and spinning of 10 kHz. Adamantane was used as reference (signal at 38.3 ppm). Data analysis was carried out using MestReNova software.

2.2.6. Isothermal stress testing (IST)

RA and the BMs were accurately weighed in glass vials. To each vial, 10% (w/w) of water was added and mixed using a glass capillary. All vials were subsequently sealed and stored in an oven at 50 °C for three weeks. RA in the BMs were quantitated by liquid chromatography (LC). The LC analysis was performed on a Shimadzu LC (LC10) coupled to UV detector. The stationary phase was a Perkin reversed-phase C18 column (150 × 4.6 mm; particle size, 5 μm), protected by C18 guard column. The mobile phase was composed of (A) acidified water (0.1% trifluoroacetic acid; pH 2.0; 75%) and (B) acidified acetonitrile (0.1% trifluoroacetic acid; 25%) at an isocratic flow rate of 1.0 mL min^{-1}. The wavelength of the detector was 330 nm, the injection volume was 10 μL and the temperature was 35 °C (Veras et al., 2019).

2.2.7. Statistical analysis

Statistical data analyses were performed using a Student's t-test ($p < 0.05$) for DSC and IST data. Cluster analysis (CA) and Pearson's correlation were applied to FTIR data. Calculations were performed using the Minitab 17 and GraphPad Prism 6 programs.

3. Results and discussion

3.1. Differential scanning calorimetry (DSC)

The RA DSC curve shows one endothermic thermal event at approximately at 171.37 °C related to its melting point and over 200 °C starts its thermal decomposition, which is in agreement with the values reported in literature (Alagawany et al., 2017; Veras et al., 2019) (Fig. 2). The DSC curves of HPMC, MCC, PVP and CCS show one thermal event at 58.30, 59.75, 68.20 and, 62.39 °C, respectively, corresponding to the dehydration and over 250 °C starts their thermal decomposition (De O. Porfírio et al., 2015; Pereira et al., 2014). The LAC curve demonstrates three endothermic events related to dehydration (144.38 °C), melting point (216.11 °C), and thermal decomposition (240.31 °C), respectively (Pereira et al., 2014). TALC shows no events in DSC analysis. The MgSTE curve also shows three endothermic events, related to loss of water (83.64 °C), dehydration (91.31 °C) and melting point (111.40 °C). Over 300 °C starts its thermal decomposition (Rao et al., 2005) (Fig. S1 and Table S1, Supplementary material).

The thermal profile of RA does not overlap with any thermal event of excipients; thus, if no interaction or incompatibility occurs, RA/excipients curves are expected to be the superposition of both thermal profiles (Fig. 3). The peak of temperature (T_{peak}), onset transition temperature (T_{onset}) and enthalpy (ΔH) of RA and it in BMs are summarized in Table 2. Variations in the values of these parameters indicate the presence of interaction or incompatibility.

Concerning excipients, the DSC curves for the BMs with HPMC, MCC, PVP and CCS show reduction of the dehydration T_{peak} value, which is associated to the lower water content in BMs. In the curves of BMs containing LAC and MgSTE, the peaks related to their dehydration and melting point were shifted (Table S1, Fig. 3).

RA melting point seems to be preserved in all BMs; however, the Student's t-test analysis indicates statistical differences (Table 2). BMs with LAC and CCS presented statistical decrease in T_{onset} value, whereas MgSTE was the only excipient to increase the T_{onset} of RA; this increase was also reported in a study by Daniel et al. (2013), in which the compatibility of risperidone with MgSTE was assessed. BMs with LAC and CCS showed statistical differences in RA T_{peak} value, and BMs containing HPMC, LAC and MgSTE demonstrated statistical differences in RA ΔH value.

There were not observed any unusual peaks in BMs DSC curves, but the alterations on RA and excipients peaks temperature and RA ΔH suggest the presence of a physical interaction in the BMs with
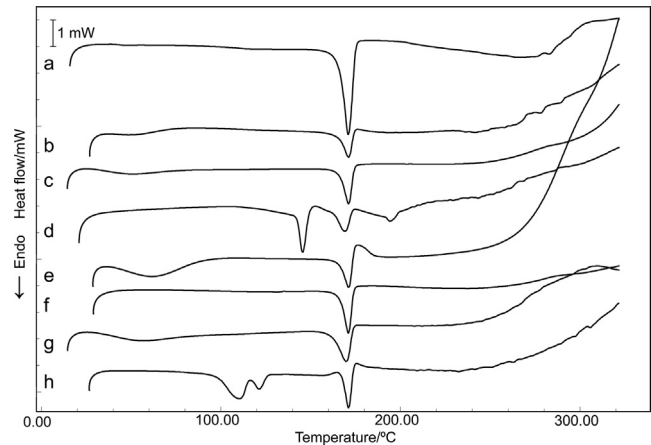
Fig. 3. DSC curves of (a) RA, (b) RA/HPMC BM, (c) RA/MCC BM, (d) RA/LAC BM, (e) RA/PVP BM, (f) RA/TALC BM, (g) RA/CCS BM and (h) RA/MgSTE.

Table 2
Temperatures and ΔH values for RA in pure form and in BMs.

Samples	T_{onset} (°C)	T_{peak} (°C)	ΔH (J g^{-1})
RA	166.68 ± 0.17[a]	171.37 ± 0.04[a]	142.29 ± 14.70[a*]
RA/HPMC	166.15 ± 0.38[a]	171.26 ± 0.16[a]	52.43 ± 4.35[b]
RA/MCC	166.35 ± 0.08[a]	171.23 ± 0.06[a]	67.86 ± 1.25[a]
RA/LAC	162.95 ± 0.48[b]	168.98 ± 0.49[b]	28.53 ± 6.32[b]
RA/PVP	166.40 ± 0.08[a]	171.31 ± 0.11[a]	56.67 ± 2.03[a]
RA/TALC	166.48 ± 0.19[a]	171.05 ± 0.09[a]	66.84 ± 6.83[a]
RA/CCS	161.95 ± 0.15[b]	169.46 ± 0.23[b]	60.70 ± 5.40[a]
RA/MgSTE	167.35 ± 0.27[a]	171.03 ± 0.13[a]	50.62 ± 1.64[b]

Samples with the same letter were not statistically different to RA sample ($p < 0.05$).
*The value used to Student's t-test was the half of ΔH for RA (71.15 ± 7.35).

HPMC, LAC, CCS and MgSTE, which can be attributed to the effect of temperature, presence of impurities and possible partial miscibility between RA and excipient (Chadha and Bhandari, 2014; Pani et al., 2012). Based on the results of DSC analyses, BMs with HPMC, LAC, CCS and MgSTE were submitted to TG analyses.

3.2. Thermogravimetry (TG)

By TG and DTG curves, RA was thermally stable up to 200 °C, corroborating the DSC results. Its decomposition occurs in two steps, the first at 297.69 °C ($\Delta m = 20.38\%$) and the second at 380.62 °C ($\Delta m = 35.17\%$). Above 670 °C, RA showed a gradual mass loss until 900 °C (Fig. 2 and Table 3). The TG curves of HPMC, LAC, CCS and MgSTE have the first thermal event related to dehydration as showed by DSC. The decomposition events of each excipient are described in Fig. S2 and Table S2 Supplementary Material (De O. Porfírio et al., 2015; Pereira et al., 2014).

Variations in the shape of TG curves, mass loss, temperatures of thermal events or appearance of new thermal events are indicative of interaction or incompatibilities between drug and excipient. In the TG curve of BMs, the first thermal event corresponds to the dehydration of the excipients, with temperatures and mass loss values lower than original components (Fig. 4A). Corresponding to RA, its first decomposition event, apparently, is present with slight change in the BMs with HPMC and LAC. In the RA/MgSTE BM, the first thermal event of RA is visualized, but shows a shift to lower temperature, while in RA/CCS BM all thermal events were related to excipient. The second decomposition event of RA was not present in any TG curves of BMs.

Though a RA thermal event is suggested in some BMs, except to CCS and the dehydration event for the other excipients, the TG
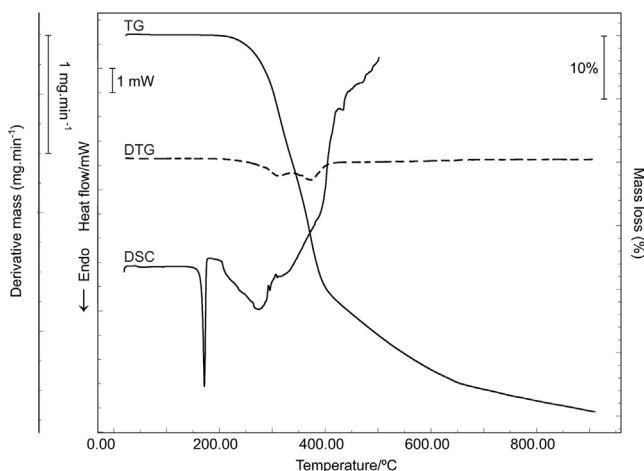
Fig. 2. DSC, TG and DTG curves of RA.

Table 3
Thermal events for RA and BMs.

Samples	First event			Second event			Third event			Fourth event		
	T_{onset} (°C)	T_{peak} (°C)	Δm(%)	T_{onset} (°C)	T_{peak} (°C)	Δm(%)	T_{onset} (°C)	T_{peak} (°C)	Δm(%)	T_{onset} (°C)	T_{peak} (°C)	Δm(%)
RA	274.73	297.69	20.38	358.04	380.62	35.17	–	–	–	–	–	–
RA/HPMC	32.21	37.21	2.89	248.43	296.41	50.47	558.36	650.61	37.75	–	–	–
RA/LAC	139.21	149.68	2.55	199.31	213.02	4.29	254.71	294.88	48.75	–	–	–
RA/CCS	38.45	59.62	4.71	281.57	315.32	51.16	775.21	812.32	17.02	–	–	–
RA/MgSTE	52.75	71.84	2.96	222.55	264.19	30.31	359.58	366.50	17.25	445.75	456.82	17.29
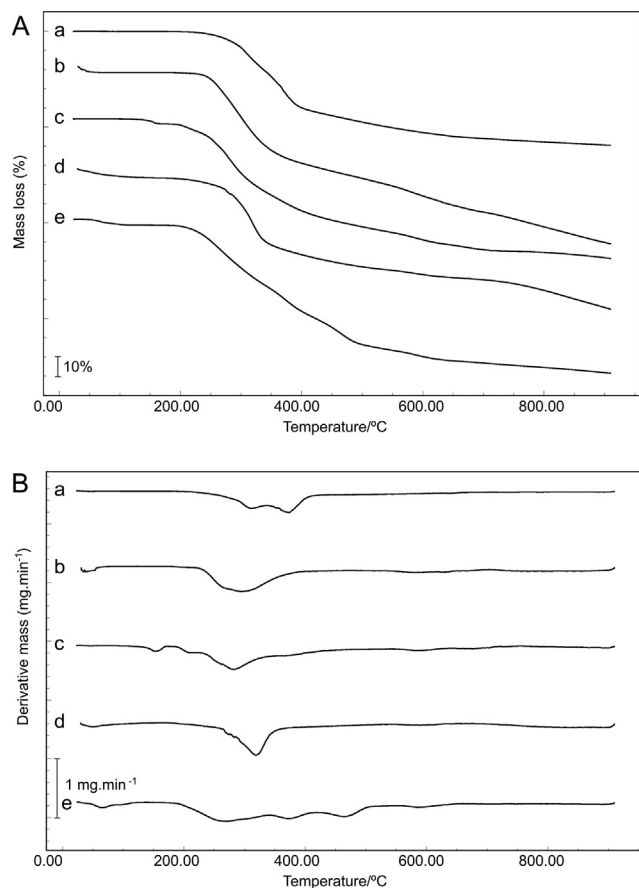
Fig. 4. TG (A) and DTG (B) curves of (a) RA, (b) RA/HPMC BM, (c) RA/LAC BM, (d) RA/CCS BM and (e) RA/MgSTE.

curves of BMs were not a superposition of RA and excipients thermal events, which was confirmed by DTG curves, also showing new thermal events (Fig. 4B), demonstrating the presence of physical interaction and suggesting chemical incompatibility.

In DSC and TG analyses, the samples are submitted to high temperatures and possible may not undergo through interactions or incompatibilities at room temperature, resulting in misleading or inconclusive results (Chadha and Bhandari, 2014), which require further analyses by non-thermal methods.

3.3. Fourier-transformed infrared (FTIR)

The FTIR spectrum for RA shows bands at: 3519, 3454 and 3397 cm^{-1} related to phenolic –OH stretching frequency; 3170 cm^{-1} related to C—H stretching frequency; 1725 and 1707 cm^{-1} related to C=O stretching frequency; 1646 cm^{-1} related to C=C stretching frequency; 1618 and 1516 cm^{-1} related to aromatic C—C stretching frequency; 1464 cm^{-1} related to CH$_2$ bending; 1285–1076 cm^{-1} related to aromatic C—H bending or C—O stretching; 971 cm^{-1} H—C(=C) bending; and 852–689 cm^{-1} aromatic C—H bending (Fig. 5) (Veras et al., 2019). The spectra for the excipients are given in Fig. S3 Supplementary Material. Modifications in the bands of the drug as broadening or intensity and occurrence of new bands are suggestive of interaction (Pereira et al., 2014).

At first glance, the FTIR spectra for the BMs show overlapping of RA and excipients bands, suggesting no chemical incompatibilities; however, in the BMs with TALC and MgSTE, RA bands related to phenolic —OH, C=O, aromatic C—C and aromatic C—H are weakly visible (Fig. 5). For deeper analysis of possible interactions between RA and the respective BMs, FTIR spectra data were submitted to cluster analysis (CA) and Pearson's correlation statistical analysis.

CA represents a statistical exploratory approach used to verify the existence of similar behavior between observations in relation to determined variables, creating groups or clusters that demonstrate internal homogeneity (Fávero and Belfiore, 2017). CA using the complete linkage Euclidean distance demonstrates that RA and RA/LAC BM had the highest similarity (>99.81%). The cluster corresponding to RA and BMs with HPMC, MCC, PVP and CCS presents 92.94% similarity, demonstrating RA profile maintenance and compatibility. In contrast, RA/MgSTE and RA/TALC BMs had a similarity of 76.76% and 63.65%, respectively, compared to RA cluster, showing a heterogeneous profile (Fig. 6).

Pearson's correlation measures the degree of linear relationship between two metric variables, with ranges from −1.00 to 1.00 (Fávero and Belfiore, 2017). The results of Pearson's correlation confirm the results obtained by CA, in which the BMs with HPMC, MCC, LAC, PVP and CCS presented correlations higher than 0.891, while TALC (r = 0.464) and MgSTE (r = 0.543) showed the lowest correlations (Fig. 7).

CA and Pearson's correlation values close to 50% and 0.50, respectively, were expected, demonstrating the simple mixture between two components; however, this did not occur. An aspect that must be take into account is the molecular weight of each component. HPMC, MCC, PVP and CCS have a high molecular weight, whereas TALC (379.26 g/mol) and MgSTE (591.26 g/mol) have a molecular weight close to RA (360.31 g/mol); thus, the differences in numbers of mols of each component in BM could affect the FTIR analysis.

Although the BMs with TALC and MgSTE results in CA and Pearson's correlations values close to those expected, the decrease in RA bands intensity indicates some interaction that can be associated with surface adsorption feature of TALC and MgSTE (Panakanti and Narang, 2012). The adsorption of atenolol on TALC surface has shown to promote shift, disappearance or intensity decrease in the drug's bands (Li et al., 2015). Another hypothesis to justify the decrease in bands intensity is that RA may quelate metallic ions present in the excipient. A bathochromic shift can occur due to an increase of the conjugate system, since stable complexes could be formed between RA hydroxyl moieties and the
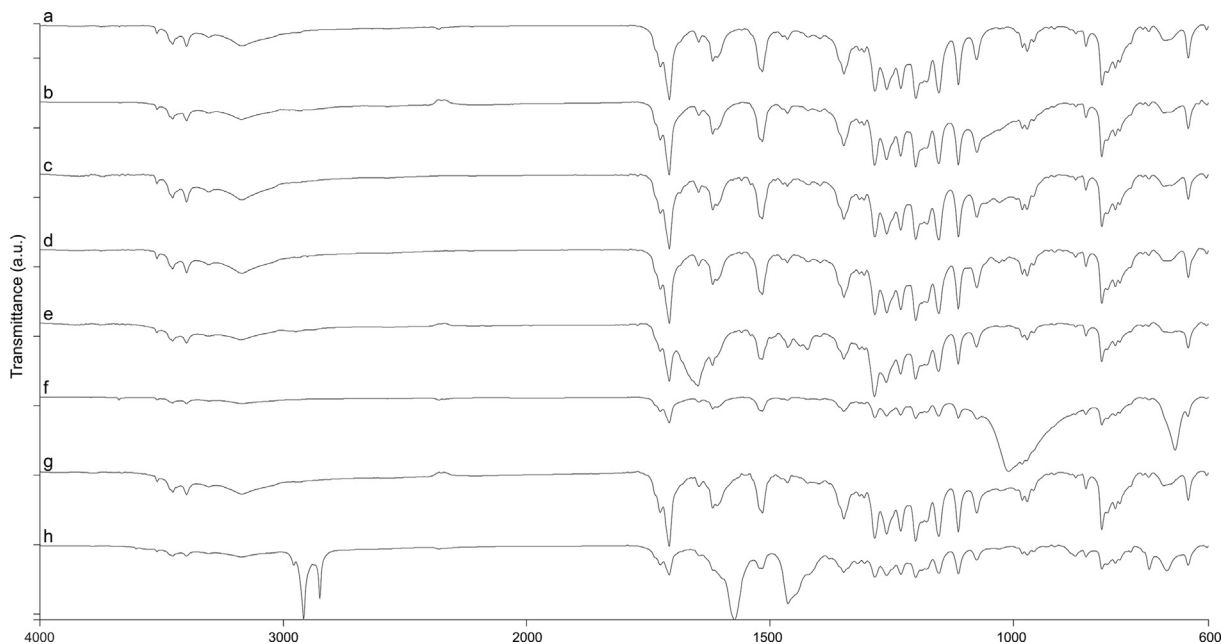
Fig. 5. FTIR spectra of (a) RA, (b) RA/HPMC BM, (c) RA/MCC BM, (d) RA/LAC BM, (e) RA/PVP BM, (f) RA/TALC BM, (g) RA/CCS BM and (h) RA/MgSTE.
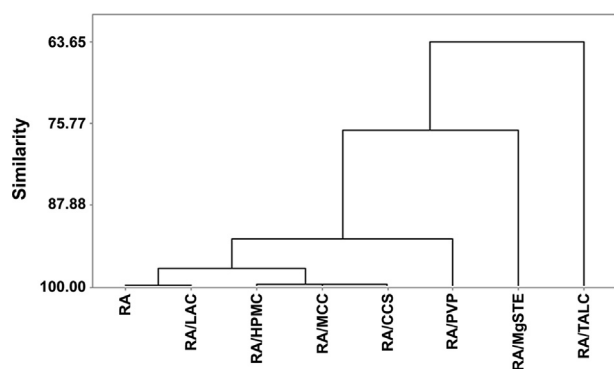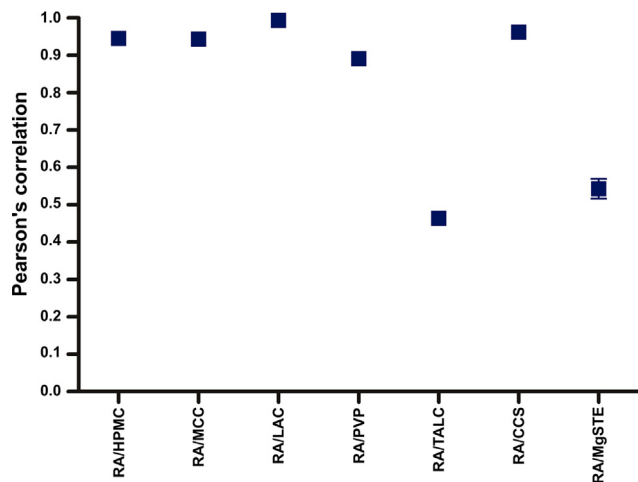

Fig. 6. Dendrogram for RA and BMs.

Fig. 7. Plot of the Pearson's correlation (r) of BMs.

metal ions (De Souza and De Giovani, 2005; Ghosh et al., 2015). Hence, in room temperature, by FTIR, RA undergo through physical interaction with TALC and MgSTE. In the attempt to evaluate these two BMs by other spectroscopic technique, ssNMR analysis was performed to further study.

3.4. Solid-state nuclear magnetic resonance (ssNMR)

ssNMR technique indicates the occurrence of interaction or incompatibility between drug and excipient in the solid state through shifts in ^{13}C signals due to change in electron density (Chadha and Bhandari, 2014).

The RA molecular structure has eighteen carbons, but ssNMR spectrum of RA shows, specifically, only eight, corresponding to two carboxylic acid (C9 e C9'), three aromatic (C1, C1' e C4'), one ethylene (C8) and two aliphatic (C7' e C8') carbons (Fig. S4). This occurs because ssNMR technique presents broadness of the lines translating in low sensitivity and resolution, resulting in overlapping signals (Skotnicki et al., 2015). Therefore, other RA carbon signals could be in the same chemical shift range corresponding to one carbon signal in ssNMR spectrum. This could occurs mainly in RA aromatic carbons, which present close signals, as C3, C4, C3' and C4' ranging 143.89–148.33 ppm; C1, C6, C1' and C6' ranging 120.41–127.87 ppm; and C2, C5, C2' and C5' ranging 113.03–116.19 ppm. (Wang et al., 2015). The application of peak analysis algorithm (global spectral deconvolution) in ssNMR spectrum of RA showed other three carbons signals at 123.76, 144.12, and 145.78 ppm, corresponding to C6, C7 and C3' (Fig. 8 and Table 4), respectively, demonstrating signal overlapping.

TALC did not present any signals in deconvoluted ssNMR spectrum, since there is no carbons in its chemical structure, while in the deconvoluted ssNMR spectrum of BM RA/MgSTE, MgSTE shows three signal at 13.72, 23.21, and 32.61 ppm, corresponding to its hydrocarbon chain, and two at 178.88 and 185.38 related to its carboxylic acid (Pisklak et al., 2016). The RA carbon profile was maintained in both BMs, except for RA C7' in RA/MgSTE BM, which was overlapped by MgSTE carbon signal (Fig. 8 and Table 4). The shifts on RA signals in BMs suggest that some perturbation is occurring due to the presence of excipients. According to Pires et al. (2017) these perturbations are not considered incompatibilities, due to the fact shifts are lower than 1 ppm; thus, this could be promoted by physical interaction, most specifically, adsorption effect.
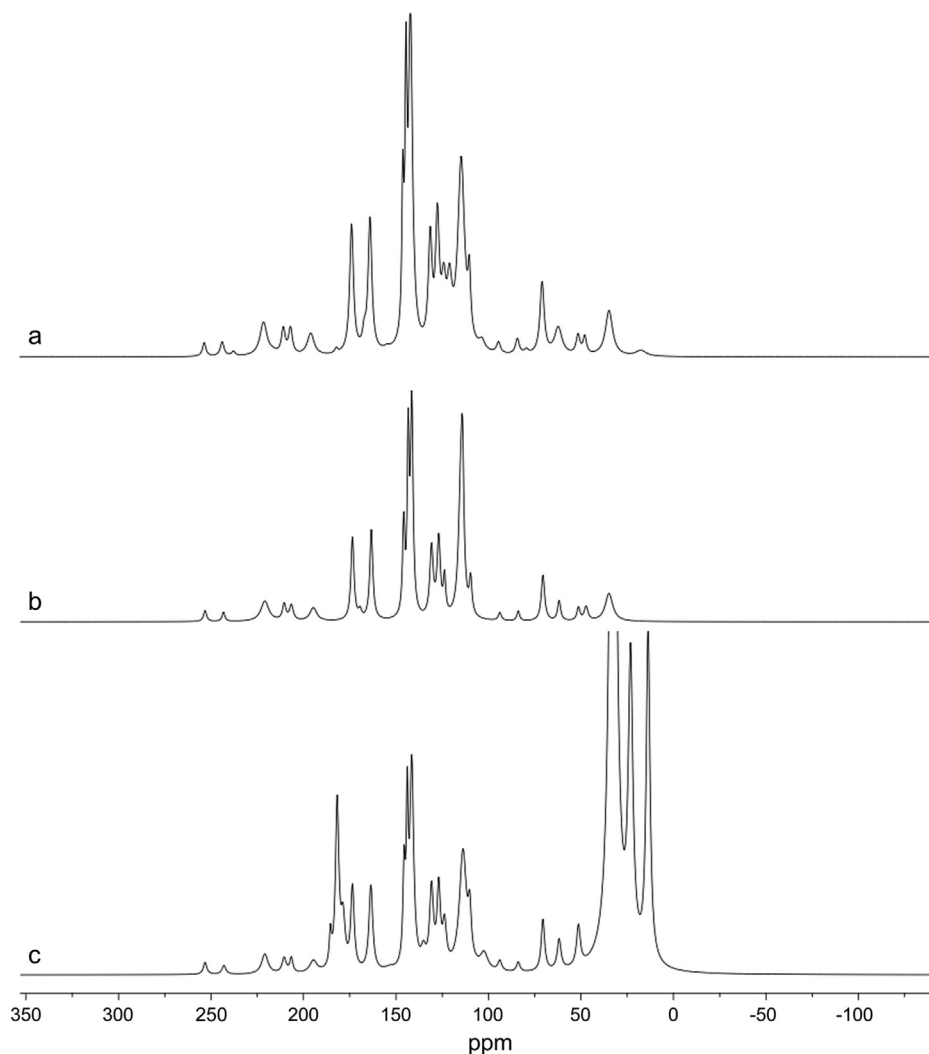
Fig. 8. Deconvoluted ssNMR spectra of (a) RA, (b) RA/TALC BM and (c) RA/MgSTE BM.

Table 4
^{13}C shifts observed for RA in pure form and in BMs.

RA carbon number	δ/ppm		
	RA	RA/TALC	RA/MgSTE
7′	34.59	34.71	–
8′	70.58	70.50	70.58
8	114.76	115.02	114.58
6	123.76	123.78	123.84
1	126.96	126.89	126.84
1′	130.86	130.72	130.80
4′	141.74	141.61	141.67
7	144.12	143.38	143.89
3′	145.78	145.81	145.52
9	163.53	163.41	163.48
9′	173.70	173.50	173.57

Besides, no unexpected signals appeared in spectra, suggesting chemical compatibility, corroborating with FTIR data.

3.5. Isothermal stress testing (IST)

The conditions used in IST provide an environment that accelerates the drug/excipients reactions. The physical interaction or chemical incompatibility between drug and excipient are determinates based on changes on visual aspects and drug content by LC method (Kaur and Sinha, 2018). BMs that were not exposed to water or heat were set as a control for IST method, which demonstrated no physical change and no significant loss of RA content (data not shown).

According to IST assay, RA was stable, presenting no significant physical change or loss of content, supporting the results reported by Razboršek (2011). Nevertheless, the stressed BMs presented physical change and the loss of RA content showed statistical differences, except to MCC. RA/CCS and RA/MgSTE BMs demonstrate

Table 5
RA content and physical changes of RA in the presence of excipients.

Samples	Stressed sample	
	RA content (%)	Physical change
RA	99.50 ± 0.45[a]	Yes
RA/HPMC	101.99 ± 0.32[b]	Yes
RA/MCC	100.78 ± 1.13[a]	Yes
RA/LAC	100.52 ± 0.60[b]	Yes
RA/PVP	98.35 ± 0.34[b]	Yes
RA/TALC	100.70 ± 1.25[b]	Yes
RA/CCS	84.07 ± 1.92[b]	Yes
RA/MgSTE	70.67 ± 0.96[b]	Yes

Samples with the same letter have no statistical difference to RA sample ($p < 0.05$).

Table 6
Summary of compatibility study results.

Excipient	DSC	TG/DTG	FTIR	ssNMR	IST
HPMC	+	+	−	NA	−
MCC	−	NA	−	NA	−
LAC	+	+	−	NA	−
PVP	−	NA	−	NA	−
TALC	−	NA	+	+	−
CCS	+	+	−	NA	+
MgSTE	+	+	+	+	+

− No interaction/incompatibility; + Interaction/incompatibility; NA: not analyzed.

the highest loss of RA content (>15%) (Table 5), indicating chemical incompatibility.

A feature that could explain the results is microenvironmental pH of the BMs in the presence of water. Excipients with ionizable functional groups, such as CCS and MgSTE, act as pH modifiers, and can change the pH its surroundings, influencing drug degradation (Badawy and Hussain, 2007; Narang et al., 2012). CCS and MgSTE present a surface pH at solid state of 4.80 and 5.12–6.80, and pH in solution of 5.40 and 9.10–9.20, respectively (Govindarajan et al., 2015; Scheef et al., 1998). RA is a strong acid substance with low pKa, being chemically susceptible to alterations of neutral pH (Danaf et al., 2016).

Compatibility studies of atorvastatin calcium and moexipril hydrochloride in solid state have demonstrated their degradation when combined with CCS and MgSTE, and submitted to temperatures above 25 °C and moisture (Govindarajan et al., 2015; Gu et al., 1990). The basic pH of MgSTE has been reported as a cause of degradation of several other drugs as acetylsalicylic acid, ibuprofen, quinapril and drotaverine hydrochloride (Li and Wu, 2014). The presence of impurities, as magnesium oxide (MgO) with MgSTE and monochloroacetate with CCS, and heavy metals in both excipients, are also related to drug degradation (Bharate et al., 2010; Wu et al., 2011).

Data presented in Table 6 indicate that RA undergo interaction/incompatibility when mixed with HPMC, LAC, TALC, CCS, and MgSTE. Specifically, HPMC and LAC in thermal analyses; TALC in non-thermal analyses; and CCS and MgSTE both in thermal and non-thermal analyses. These results suggest that HPMC and LAC only promoted physical-chemical alterations on RA due to the use of high temperatures required for the technique.

Daniel et al. (2013) described interactions between risperidone and excipients by DSC, while in the analyses of the BMs by FTIR before and after heating, chemical incompatibilities were only detected after heating during DSC experiments. Thus, HPMC and LAC have their use in combination with RA limited to pharmaceutical dosage forms production techniques that do not require high temperature, since in IST, using temperature above room temperature but lower than DSC and TG analyses, no chemical incompatibility were detected.

Interactions between RA and TALC were demonstrated by FTIR spectra, suggestive of adsorption effect, and did not promote chemical degradation on RA by ssNMR and IST. Despite the adsorption of drug on excipient surface in pharmaceutical solid form can affect the drug release, influencing in its activity or bioavailability, according to literature, TALC do not promote significant changes on drug release (Dürig and Fassihi, 1997; Panakanti and Narang, 2012).

MgSTE and CCS play as the most critical excipients to the development of pharmaceutical dosage forms with RA, since they presented chemical incompatibility in IST assay. IST test allows to evaluate the excipients physicochemical characteristics, as well as the effects of temperature and presence of water on the drug stability (Serajuddin et al., 1999). Since similar conditions are used to predict the stability of a pharmaceutical dosage form, in acceler-

ated and long-time analyses, the results show that CCS and MgSTE could decrease the shelf-life of the RA in final product (Qiu et al., 2009). MCC and PVP did not present any interaction or incompatibility with RA by the methods applied.

4. Conclusion

The compatibility study of drug and excipients is important to predict the stability of the drug in the final pharmaceutical product. This study demonstrated for the first time that RA was compatible with MCC and PVP. HPMC, LAC, CCS and MgSTE promoted physical interaction and chemical incompatibilities by thermal methods. TALC and MgSTE demonstrated physical interaction by FTIR and ssNMR, and CCS and MgSTE promoted chemical degradation by IST. The high temperature and presence of water are factors that influence physical-chemical changes on RA with some excipients. These features must be taken into account in the development of a solid dosage form containing RA.

Appendix A. Supplementary material

Supplementary data to this article can be found online at https://doi.org/10.1016/j.jsps.2019.09.010.

References

Alagawany, M., Abd El-Hack, M.E., Farag, M.R., Gopi, M., Karthik, K., Malik, Y.S., Dhama, K., 2017. Rosmarinic acid: modes of action, medicinal values and health benefits. Anim. Heal. Res. Rev. 1–10. https://doi.org/10.1017/S1466252317000081.

Amoah, S.K.S., Sandjo, L.P., Kratz, J.M., Biavatti, M.W., 2016. Rosmarinic acid – pharmaceutical and clinical aspects. Planta Med. 82, 388–406.

Badawy, S.I., Hussain, M., 2007. Microenvironmental pH modulation in solid dosage forms. J. Pharm. Sci. 96, 948–959. https://doi.org/10.1002/jps.

Bezerra, G.S.N., Pereira, M.A.V., Ostrosky, E.A., Barbosa, E.G., de Moura, M. de F.V., Ferrari, M., Aragão, C.F.S., Gomes, A.P.B., 2017. Compatibility study between ferulic acid and excipients used in cosmetic formulations by TG/DTG, DSC and FTIR. J. Therm. Anal. Calorim. 127, 1683–1691. https://doi.org/10.1007/s10973-016-5654-9.

Bharate, S.S., Bharate, S.B., Bajaj, A.N., 2010. Interactions and incompatibilities of pharmaceutical excipients with active pharmaceutical ingredients : a comprehensive review. J. Excipients Food Chem. 1, 3–26.

Campos, D.A., Madureira, A.R., Gomes, A.M., Sarmento, B., Pintado, M.M., 2014. Optimization of the production of solid Witepsol nanoparticles loaded with rosmarinic acid. Colloids Surf. B Biointerfaces 115, 109–117. https://doi.org/10.1016/j.colsurfb.2013.10.035.

Chadha, R., Bhandari, S., 2014. Drug-excipient compatibility screening-Role of thermoanalytical and spectroscopic techniques. J. Pharm. Biomed. Anal. 87, 82–97. https://doi.org/10.1016/j.jpba.2013.06.016.

Danaf, N. Al, Melhem, R.A., Assaf, K.I., Nau, W.M., Patra, D., 2016. Photophysical properties of neutral and dissociated forms of rosmarinic acid. J. Lumin. 175, 50–56. https://doi.org/10.1016/j.jlumin.2016.02.011.

Daniel, J.S.P., Veronez, I.P., Rodrigues, L.L., Trevisan, M.G., Garcia, J.S., 2013. Risperidone - solid-state characterization and pharmaceutical compatibility using thermal and non-thermal techniques. Thermochim. Acta 568, 148–155. https://doi.org/10.1016/j.tca.2013.06.032.

De O. Porfírio, L., Costa, A.A., Conceição, R.R., De O. Matos, T., Almeida, E.D.P., Sarmento, V.H.V., Araújo, A.A.S., De S. Nunes, R., Lira, A.A.M., 2015. Compatibility study of hydroxypropylmethylcellulose films containing zidovudine and lamivudine using thermal analysis and infrared spectroscopy. J. Therm. Anal. Calorim. 120, 817–828. https://doi.org/10.1007/s10973-014-3938-5.

de Oliveira, G.G.G., Feitosa, A., Loureiro, K., Fernandes, A.R., Souto, E.B., Severino, P., 2017. Compatibility study of paracetamol, chlorpheniramine maleate and phenylephrine hydrochloride in physical mixtures. Saudi Pharm. J. 25, 99–103. https://doi.org/10.1016/j.jsps.2016.05.001.

De Souza, R.F.V., De Giovani, W.F., 2005. Synthesis, spectral and electrochemical properties of Al(III) and Zn(II) complexes with flavonoids. Spectrochim. Acta - Part A Mol. Biomol. Spectrosc. 61, 1985–1990. https://doi.org/10.1016/j.saa.2004.07.029.

Dürig, T., Fassihi, R., 1997. Mechanistic evaluation of binary effects of magnesium stearate and talc as dissolution retardants at 85% drug loading in an experimental extended- release formulation. J. Pharm. Sci. 86, 1092–1098. https://doi.org/10.1021/js970052v.

Fachel, F.N.S., Schuh, R.S., Veras, K.S., Bassani, V.L., Koester, L.S., Henriques, A.T., Braganhol, E., Teixeira, H.F., 2019. An overview of the neuroprotective potential of rosmarinic acid and its association with nanotechnology-based delivery systems: A novel approach to treating neurodegenerative disorders. Neurochem. Int. 122, 47–58. https://doi.org/10.1016/j.neuint.2018.11.003.

Fávero, L., Belfiore, P., 2017. Manual de análise de dados: Estatística de modelagem multivariada com Excel®, SPSS® and Stata®. Elsevier, Rio de Janeiro.

Ghosh, N., Chakraborty, T., Mallick, S., Mana, S., Singha, D., Ghosh, B., Roy, S., 2015. Synthesis, characterization and study of antioxidant activity of quercetin-magnesium complex. Spectrochim. Acta - Part A Mol. Biomol. Spectrosc. 151, 807–813. https://doi.org/10.1016/j.saa.2015.07.050.

Govindarajan, R., Landis, M., Hancock, B., Gatlin, L.A., Suryanarayanan, R., Shalaev, E. Y., 2015. Surface acidity and solid-state compatibility of excipients with an acid-sensitive API: Case study of atorvastatin calcium. AAPS PharmSciTech 16, 354–363. https://doi.org/10.1208/s12249-014-0231-7.

Gu, L., Strickley, R.G., Chi, L.H., Chowhan, Z.T., 1990. Drug-excipient incompatibility studies of the dipeptide angiotensin-converting enzyme inhibitor, moexipril hydrochloride: dry powder vs wet granulation. Pharm. Res. An Off. J. Am. Assoc. Pharm. Sci. https://doi.org/10.1023/A:1015871406549.

Kaur, R., Sinha, V.R., 2018. Use of thermal and non thermal techniques for assessing compatibility between mirtazapine and solid lipids. J. Pharm. Biomed. Anal. 161, 144–158. https://doi.org/10.1016/j.jpba.2018.08.041.

Li, J., Wu, Y., 2014. Lubricants in pharmaceutical solid dosage forms. Lubricants 2, 21–43. https://doi.org/10.3390/lubricants2010021.

Li, Z., Fitzgerald, N.M., Lv, G., Jiang, W.-T., Wu, L., 2015. Adsorption of atenolol on talc: an indication of drug interference with an excipient. Adsorpt. Sci. Technol. 33, 379–392. https://doi.org/10.1260/0263-6174.33.4.379.

Madureira, A.R., Campos, D.A., Fonte, P., Nunes, S., Reis, F., Gomes, A.M., Sarmento, B., Pintado, M.M., 2015. Characterization of solid lipid nanoparticles produced with carnauba wax for rosmarinic acid oral delivery. RSC Adv. 5, 22665–22673. https://doi.org/10.1039/C4RA15802D.

Narang, A.S., Desai, D., Badawy, S., 2012. Impact of excipient interactions on solid dosage form stability. Pharm. Res. 29, 2660–2683. https://doi.org/10.1007/s11095-012-0782-9.

Panakanti, R., Narang, A.S., 2012. Impact of excipient interactions on drug bioavailability from solid dosage forms. Pharm. Res. 29, 2639–2659. https://doi.org/10.1007/s11095-012-0782-9.

Pani, N.R., Nath, L.K., Acharya, S., Bhuniya, B., 2012. Application of DSC, IST, and FTIR study in the compatibility testing of nateglinide with different pharmaceutical excipients. J. Therm. Anal. Calorim. 108, 219–226. https://doi.org/10.1007/s10973-011-1299-x.

Pereira, M.A.V., Fonseca, G.D., Silva-Júnior, A.A., Fernandes-Pedrosa, M.F., De, M., Barbosa, E.G., Gomes, A.P.B., Dos Santos, K.S.C.R., 2014. Compatibility study between chitosan and pharmaceutical excipients used in solid dosage forms. J. Therm. Anal. Calorim. 116, 1091–1100. https://doi.org/10.1007/s10973-014-3769-4.

Pires, S.A., Mussel, W.N., Yoshida, M.I., 2017. Solid-state characterization and pharmaceutical compatibility between citalopram and excipients using thermal and non-thermal techniques. J. Therm. Anal. Calorim. 127, 535–542. https://doi.org/10.1007/s10973-016-5769-z.

Pisklak, D.M., Zielińska-Pisklak, M.A., Szeleszczuk, Ł., Wawer, I., 2016. 13C solid-state NMR analysis of the most common pharmaceutical excipients used in solid drug formulations, Part I: Chemical shifts assignment. J. Pharm. Biomed. Anal. 122, 81–89. https://doi.org/10.1016/j.jpba.2016.01.032.

Qiu, Y., Chen, Y., Zhang, G.G., Liu, L., Porfer, W.R., 2009. Developing Solid Oral Dosage Forms. Academic Press.

Rao, K.P., Chawla, G., Kaushal, A.M., Bansal, A.K., 2005. Impact of solid-state properties on lubrication efficacy of magnesium stearate. Pharm. Dev. Technol. 10, 423–437.

Razboršek, M.I., 2011. Stability studies on trans-rosmarinic acid and GC-MS analysis of its degradation product. J. Pharm. Biomed. Anal. 55, 1010–1016. https://doi.org/10.1016/j.jpba.2011.04.003.

Rojek, B., Wesolowski, M., Suchacz, B., 2013. Detection of compatibility between baclofen and excipients with aid of infrared spectroscopy and chemometry. Spectrochim. Acta - Part A Mol. Biomol. Spectrosc. 116, 532–538. https://doi.org/10.1016/j.saa.2013.07.102.

Rowe, R.C., Sheskey, P.J., Cook, W.G., Fenton, M.E., 2012. Handbook of Pharmaceutical Excipients. Pharmaceutical UK, London.

Scheef, C.A., Oelkrug, D., Schmidt, P.C., 1998. Surface acidity of solid pharmaceutical excipients III. Excipients for solid dosage forms. Eur. J. Pharm. Biopharm. 46, 209–213. https://doi.org/10.1016/S0939-6411(98)00025-3.

Serajuddin, A.T., Thakur, A.B., Ghoshal, R., Fakes, M.G., Ranadive, S., Morris, K., Varia, S., 1999. Selection of solid dosage form composition through drug-excipient compatibility testing. J. Pharm. Sci. 88, 696–704.

Skotnicki, M., Aguilar, J.A., Pyda, M., Hodgkinson, P., 2015. Bisoprolol and bisoprolol-valsartan compatibility studied by differential scanning calorimetry, nuclear magnetic resonance and X-Ray powder diffractometry. Pharm. Res. 32, 414–429. https://doi.org/10.1007/s11095-014-1471-7.

Veras, K.S., Silveira Fachel, F.N., Delagustin, M.G., Teixeira, H.F., Barcellos, T., Henriques, A.T., Bassani, V.L., Koester, L.S., 2019. Complexation of rosmarinic acid with hydroxypropyl-β-cyclodextrin and methyl-β-cyclodextrin: Formation of 2:1 complexes with improved antioxidant activity. J. Mol. Struct. 1195, 582–590. https://doi.org/10.1016/j.molstruc.2019.06.026.

Verma, R.K., Garg, S., 2005. Selection of excipients for extended release formulations of glipizide through drug-excipient compatibility testing. J. Pharm. Biomed. Anal. 38, 633–644. https://doi.org/10.1016/j.jpba.2005.02.026.

Wang, Y., Tang, J., Zhu, H., Jiang, X., Liu, J., Xu, W., Ma, H., Feng, Q., Wu, J., Zhao, M., Peng, S., 2015. Aqueous extract of Rabdosia rubescens leaves: Forming nanoparticles, targeting P-selectin, and inhibiting thrombosis. Int. J. Nanomed. 10, 6905–6918. https://doi.org/10.2147/IJN.S91316.

Wu, Y., Levons, J., Narang, A.S., Raghavan, K., Rao, V.M., 2011. Reactive impurities in excipients: profiling, identification and mitigation of drug-excipient incompatibility. AAPS PharmSciTech 12, 1248–1263. https://doi.org/10.1208/s12249-011-9677-z.